Al Azhar Bulletin of Science Vol. 29, No. 2 (December), 2018, pp. 1-6.

ELLIPSOMETRIC STUDIES OF SURFACE LAYERS FORMED ON STAINLESS STEEL MASS STANDARDS

Alaaeldin. A. Eltawil[1], N. A. Mahmoud[2], Sayed. A. Emira[3], N. N. Nagib[4], M. M. Eloker[5]

[1, 2, 3 and 4] *National institute of standard, Giza, Egypt.*
[5] *Elazhar university, physics department, faculty of science, Egypt.*

ABSTRACT

Three stainless steel mass standards of different grades each of mass 100 g were studied under normal ambient conditions by ellipsometry to determine the surface layers formed on them. The studied specimens are of grades E_1, E_2, and F_1. The factors influencing the thickness of the surface layers were discussed. It was observed that the thicknesses of formed layers on different mass standards were not equal. The estimated values of the oxide and water layers range between 1 nm and 5 nm.

1. INTRODUCTION

The SI unit of mass is the kilogram, defined as the mass of the "international prototype", a cylinder of platinum-10% iridium alloy kept at the Bureau International des Poids et Mesures (BIPM) at Sèvres, France. This is the only remaining SI unit to be defined in terms of a physical artefact. At BIPM, over sixty copies of this kilogram have been made [1], the BIPM routinely uses these copies as reference standards. Similar prototypes are held by national metrology institutes (NIS in Egypt have national prototype kilogram no.58) as national standards [2].

This standard mass is expensive, and so, beyond the next stage, stainless steel masses are used lower quality reference masses although the component elements are highly reactive [3]. Instabilities of stainless steel masses arise through surface effects. The changes at the surface of an artefact cause changes in the value of its mass. Also, the change in mass can take place by the humidity of ambient air. A number of experiments, both gravimetric and optical, have been performed to quantify the effect of humidity on the mass of metallic artefacts. Under normal environmental conditions, a water adsorped layer is formed on the surface of solids. The thickness of this adsorbed layer (nanometer range) depends, among other things, upon the humidity of the ambient air [4].

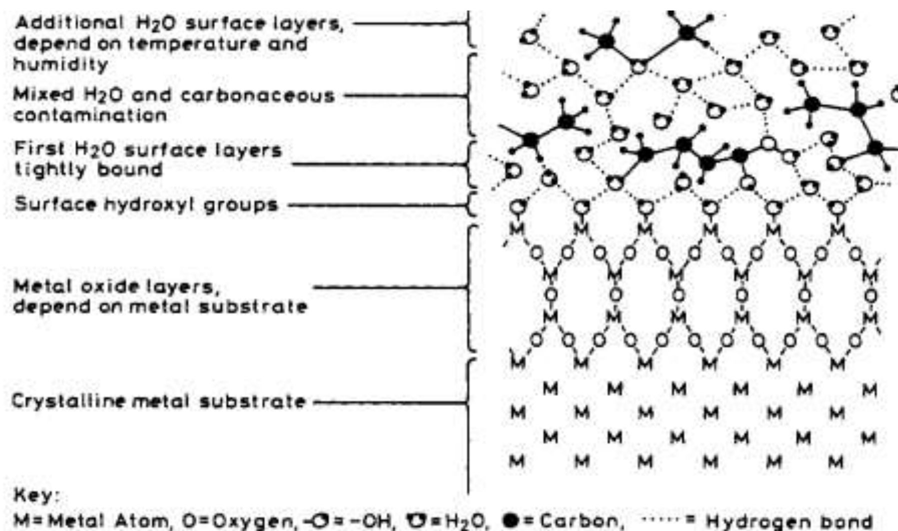

Fig.(1) Schematic diagram showing the structure of the stainless steel/air interface conjectured.

In a typical laboratory weighing environment we might expect that the surface of stainless steel will comprise the base material over which, will be a thin coherent oxide. This, in turn, will be covered with hydrocarbon contamination and some layers of chemisorbed and physisorbed water, as shown in Figure (1). As a result of the different heats of formation of the oxides of chromium, iron and nickel, and also arising from the different diffusivities involved the oxide composition has a different cations compared with the matrix, and to maintain conservation of matter, this implies that the metal layer just under the oxide differs from that of the bulk material. Bearing in mind that one monolayer of carbon, water and oxide at the surface add masses of 9 µg, 4 µg and 17 µg, respectively [5].

Surface effects on standard weights have previously been studied gravimetrically and using different surface analysis techniques, such as x-ray photoelectron spectroscopy (XPS), Thermal desorption spectroscopy (TDS), secondary ion mass spectrometry (SIMS), time-of-flight SIMS (TOF-SIMS), Auger electron spectroscopy (AES), x-ray fluorescence (XRF), scanning electron microscopy (SEM) and ellipsometry [6-12]. Each technique has its advantages and drawbacks. XPS, TDS, SIMS, TOF-SIMS, AES and XRF give information about the composition of the surface contamination layers. SEM provides morphological information of the surface at the nanometer scale and ellipsometry provides information about the contamination layer thickness.

Ellipsometry is an accurate and non-destructive technique for thin film and surface measurements. When plane polarized light is reflected from conducting surface, the reflected beam will be elliptically polarized. The state of polarization is determined by the ellipsometric parameters **Ψ** and Δ and the fundamental equation of ellipsometry is expressed as [13]:

$$\rho = \frac{\rho_p}{\rho_s} = \tan\Psi \, e^{i\Delta} \qquad (1)$$

ρ is the complex reflectivity and the parameters Δ and **Ψ** represents the phase shifts and amplitude changes on reflection for the parallel **p** and perpendicular **s** components of the electric vector. Thus, if $\boldsymbol{\delta_{ip}}$ and $\boldsymbol{\delta_{is}}$ are the phases of the **p** and **s** components respectively of the incident beam and $\boldsymbol{\delta_{rp}}$ and $\boldsymbol{\delta_{rs}}$ are the corresponding phases after reflection, then

$$\Delta = (\delta_{rp} - \delta_{rs}) - (\delta_{ip} - \delta_{is}) \qquad (2)$$

Also,

$$\tan\Psi = \left[\frac{E_{rp}}{E_{ip}}\right] \Big/ \left[\frac{E_{rs}}{E_{is}}\right] \qquad (3)$$

Where E is the amplitude of the electric vector and the subscripts have the same meaning as in Eq. (2).

Optical interference takes place if a thin film is formed on a substrate. This interference effect is used to determine the thickness of formed thin films and multilayers. Starting with the model ambient-film-substrate, fig.2, where N_0, N_1 and N_2 refer to the refractive indices of air, film and substrate respectively. The light wave reflected at the film surface (primary beam) and the light wave reflected at the film – substrate interface (secondary beam) will interfere. The film thickness d is related to phase variation (also called the film phase thickness) β by the relation [13]:

$$\beta = \frac{2\pi d}{\lambda}\left(N_1^2 - N_0^2 \sin^2\theta_0\right)^{1/2} \qquad (4)$$

Where θ_0 is the incident angle.

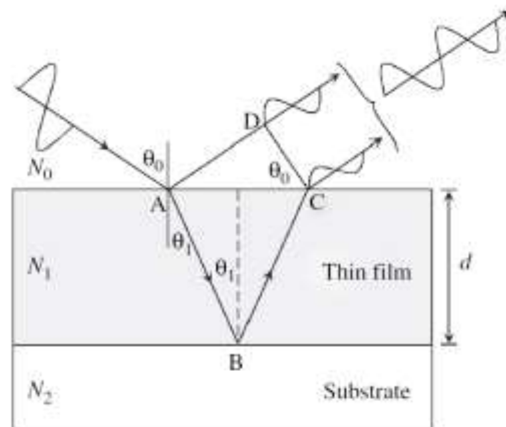

Fig.(2) Optical interference in a thin film formed on a substrate.

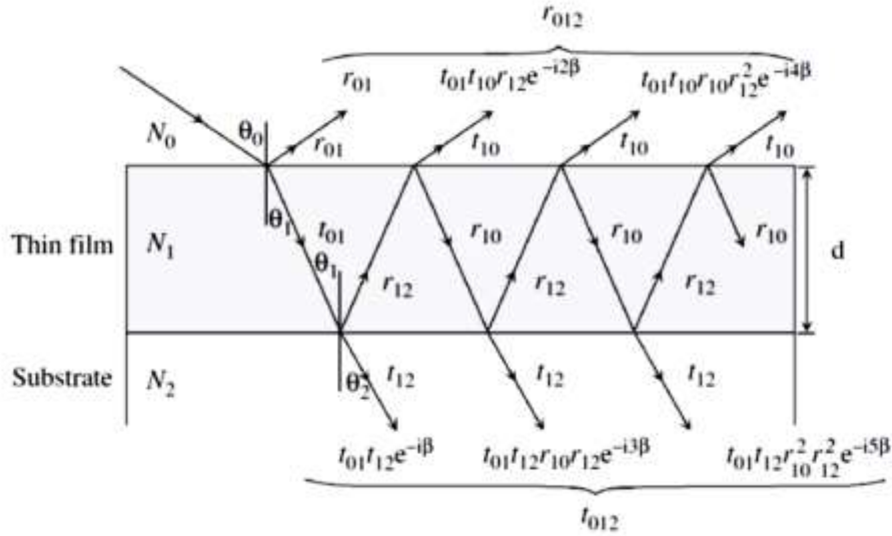

Fig. (3) optical model for an ambient/thin film/substrate structure.

The reflected and transmitted amplitudes are related to reflection and transmission coefficients by [14]:

$$r_{012} = r_{01} + t_{01}t_{10}\, r_{12}e^{-i2\beta} + t_{01}t_{10}\, r_{12}\, r_{12}^{2}e^{-i4\beta} + t_{01}t_{10}\, r_{10}^{2}r_{12}^{3}e^{-i6\beta} + \cdots \tag{5}$$

And

$$t_{012} = t_{01}t_{12}\, e^{-i\beta} + t_{01}t_{10}\, r_{10}\, r_{12}e^{-i3\beta} + t_{01}t_{12}\, r_{10}^{2}r_{12}^{2}e^{-i5\beta} + \cdots \tag{6}$$

This could be written as

$$r_{012} = \frac{\left[r_{01} + r_{12}\, e^{-i2\beta}\right]}{\left[1 + r_{01}\, r_{12}\, e^{-i2\beta}\right]} \tag{7}$$

$$t_{012} = \frac{\left[t_{01}t_{12}\, e^{-i\beta}\right]}{\left[1 + r_{01}\, r_{12}\, e^{-i2\beta}\right]} \tag{8}$$

Fresnel reflection coefficient at the air-film and the film-substrate interface for the **p** and **s** component are given by:

$$r_{01p} = {[N_1\cos\theta_0 - N_0\cos\theta_1]}/{[N_1\cos\theta_0 + N_0\cos\theta_1]} \tag{9}$$

$$r_{12p} = {[N_2\cos\theta_1 - N_1\cos\theta_2]}/{[N_2\cos\theta_1 + N_1\cos\theta_2]} \tag{10}$$

$$r_{01s} = {[N_0\cos\theta_0 - N_1\cos\theta_1]}/{[N_0\cos\theta_0 + N_1\cos\theta_1]} \tag{11}$$

$$r_{12s} = {[N_1\cos\theta_1 - N_2\cos\theta_2]}/{[N_1\cos\theta_1 + N_2\cos\theta_2]} \tag{12}$$

The angles θ_0, θ_1 and θ_2 follow Snell's law:

$$N_0\sin\theta_0 = N_1\sin\theta_1 = N_2\sin\theta_2 \tag{13}$$

Equations (9)-(12) are used to determine the reflection coefficients r_{01p}, r_{12p}, r_{01s} and r_{12s}. Solving Eq. (7) for β, we can determine the film thickness using Eq. (4)

2- EXPERIMENTAL DETAILS

The studied three mass standards E_1, E_2 and F_1 (classification according to International Organization of Legal Metrology **OIML R111**) are each of mass 100 g [15]. The highest grade of the studied standard masses is the E_1 followed by E_2 and F_1 respectively. Measurements were carried out on the flat surface of the mass standards using automatic ellipsometer type PHE-103 spectroscopic ellipsometer, Angstrom Advanced shown in figure (4). Oxide and adsorped water layers are formed on the surface of these artifacts due to several factors including surface cleanliness, surface roughness, composition, ambient temperature and environmental conditions. In the present work, the thickness of the formed oxide layer and adsorbed water layer were measured by ellipsometry in the range of wavelength from 400 nm to 800 nm.

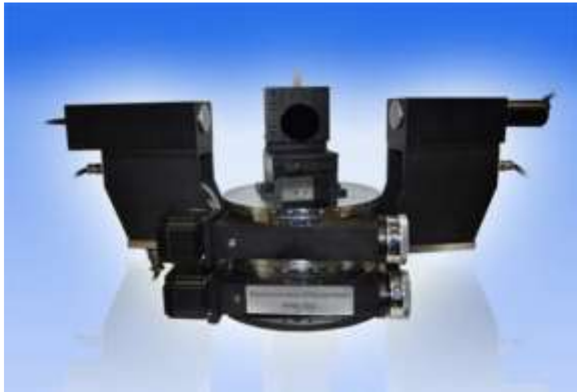

Fig. (4) PHE-103 spectroscopic ellipsometer

3- RESULTS AND DISCUSSION

Each of the studied samples was treated as a system of four components (air, water film, oxide film and sample). Measurements were carried out at temperature (19.6 ± 0.2) °C and relative humidity (55.5% ± 2%). For a system with two films, the ellipsometer measures the thickness of the film directly above the substrate, then the other film.

The estimated values of Ψ and Δ of the three mass standards are shown in figure (5, 6 and 7) and given in table (1, 2 and 3).The data of all samples show the same behaver .Where Ψ decreases by increasing wavelength in the range 400 nm-800 nm. On the other hand Δ follow opposite trend. It should be noted that the thickness of adsorbed layers depend on composition, surface roughness and frequency use of mass standards [12, 16 and17].

It is observed from figure (6) that the values of the ellipsometric angles Ψ and Δ for the mass standard E_2 where Ψ decreases from 34.25° to 31.74° as λ increases from 400 nm to 700 nm and above 700 nm it starts to increase to 31.97° at 800 nm.At the same spectral range, Δ increased from 95.95° to 125.20°.

Estimated values of n and k for the same stainless steel mass standard E_2 between 400 nm and 800 nm are presented in table (4) and Figure (8).

Table (1) values of Ψ and Δ of mass standard E_1.

λ (nm)	Ψ	Δ
400	35.70	98.57
450	35.62	100.46
500	35.45	101.83
550	35.19	103.92
600	34.93	104.28
650	34.79	106.22
700	34.61	108.63
750	34.64	109.38
800	34.56	111.83

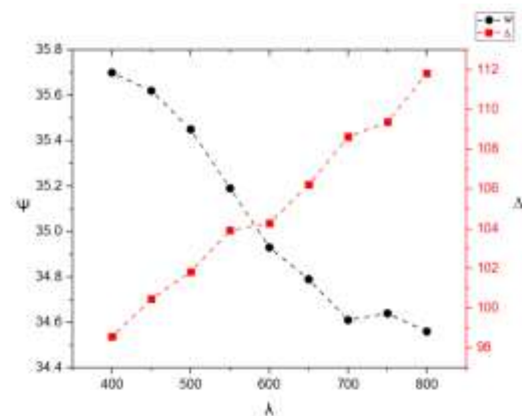

Fig. (5) variation of Ψ and Δ with the wavelength for mass standard E_1.

Table (2) values of Ψ and Δ of mass standard E_2.

λ(nm)	Ψ	Δ
400	34.25	95.95
450	33.55	102.9
500	32.84	108.25
550	32.30	112.57
600	31.97	115.78
650	31.85	118.66
700	31.74	121.13
750	31.92	122.77
800	31.97	125.20

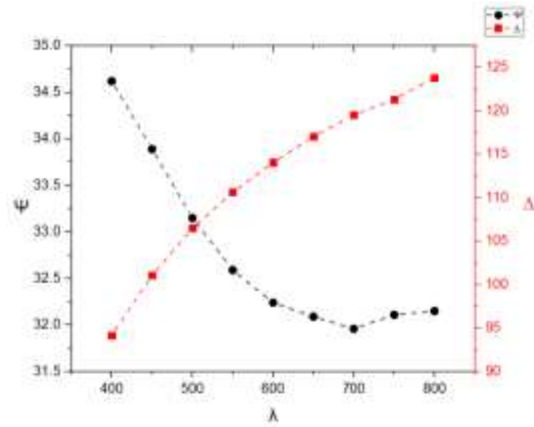

Fig. (6) variation of Ψ and Δ with the wavelength for mass standard E_2.

Table (3) values of Ψ and Δ of mass standard F_1.

λ(nm)	Ψ	Δ
400	34.62	94.18
450	33.89	101.09
500	33.15	106.5
550	32.59	110.65
600	32.24	114.07
650	32.09	117.07
700	31.96	119.53
750	32.11	121.33
800	32.15	123.82

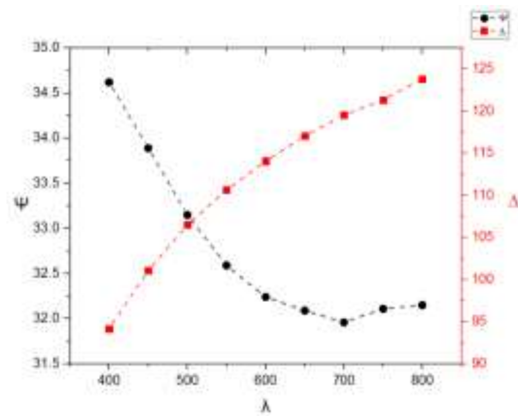

Fig. (7) variation of Ψ and Δ with the wavelength for mass standard F1.

Table (4) values of n, k of the mass standard E_2.

λ(nm)	n	k
400	1.12	2.50
450	1.34	2.80
500	1.56	3.10
550	1.76	3.20
600	1.91	3.33
650	2.06	3.48
700	2.19	3.59
750	2.26	3.71
800	2.40	3.86

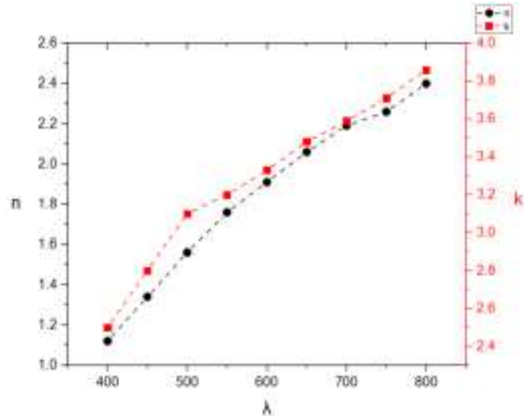

Fig. (8) dependence the optical constants of n,k for the mass standard E2on the wavelength.

Ellipsometric results for the oxide and water adsorbed film thicknesses and standard uncertainty are presented for the studied mass standards in table (5). Each value in the table is the result of the mean value of five measurements.

Table (5). thickness of the oxide and water adsorbed films

sample	Thickness of oxide film(nm)	Standard uncertaint y(nm)	Thickness of adsorbed water (nm)	Standard uncertainty(nm)
E_1	5.46	0.16	1.11	0.05
E_2	5.10	0.12	2.41	0.03
F_1	4.63	0.06	2.68	0.06

4- CONCLUSION

The thickness of contaminated layers formed on the surface of mass standard were evaluated. This is to improve the information about the change in mass standard and imperative the redefinition of the kilogram. The thickness of adsorbed water and the oxide layer was determined by ellipsometry. The obtained values were found to lay between 1 nm to 5 nm at the range of wavelength 400 nm- 800 nm at the ambient {temperature (19.6 ± 0.2) ^{o}C and relative humidity (55.5% ± 2%)}. The difference in measurement results between the present study and other studies might be caused by samples composition and conditions of measurement. In relation to this, we would also like to investigate the influence of the surface roughness and cleanliness on the amount of physical adsorption of water vapour in the future.

REFERENCES

1- P. J. Cumpson and M. P. Seah, Stability of Reference Masses IV: Growth of carbonaceous contamination on platinum-iridium alloy surfaces and cleaning by UV/ozone treatment, Metrologia,**33** (1996) 507-532.

2- P. J. Cumpson and M. P. Seah, Stability of Reference Masses 111: Mechanism and Long-term Effects of Mercury Contamination on Platinum-Iridium Mass Standards, Metrologia, **31** (1994/1995) 375-388.

3- P. J. Cumpson and M. P. Seah, Stability of Reference Masses I: Evidence for Possible Variations in the Mass of Reference Kilograms Arising from Mercury Contamination, Metrologia**, 31** (1994) 2 1-26.

4- Stuart Davidson, A review of surface contamination and the stability of standard masses, Metrologia, **40** (2003) 324-338.

5- M. P. Seah, J. H. Qiu, P. J. Cumpson and J. E. Castle, Stability of Reference Masses II: The Effect of Environment and Cleaning Methods on the Surfaces of Stainless Steel and Allied Materials, Metrologia, **31** (1994) 93-108.

6**-** P Fuchs, K Marti, G Grgic and S Russi, UV/ozone cleaning of mass standards: results on the correlation between mass and surface chemical state, Metrologia, **51** (2014) 387–393.

7- Y. Hashiguchi, K. Mizuno and M. Nagoshi, Surface Analytical Study of the Cause of Mass Gain of the Kilogram Prototype, SURFACE AND INTERFACE ANALYSIS, VOL. **20** (1993) 276-282.

8**-** D.R. Sharma, B.R. Chakraborty and M.L. Das, Comparative SIMS investigations on surface contamination of Pt–Ir alloy treated by different cleaning procedures, Applied Surface Science **135** (1998) 193–199.

9- R Hogstrom, V Korpelainen, K Riski and M Heinonen, Atomic force microscopy studies of surface contamination on stainless steel weights, Metrologia, **47**(2010) 670-676.

10- Gisele Cristiane Becher Ribas and Fernando Luis Fertonani, Thermal and electrochemical study of solid-state reaction of mercury with Pt–20% Rh alloy, J Therm Anal Calorim 104 (2011) 549–554.

11- Peter J Cumpson, Lisa W Li and Naoko Sano, Stability of Reference Masses VIII: X-Ray Fluorescence (XRF) as a Noncontact, Nondestructive Measurement Method for Trace Mercury Contamination of Platinum-Group Metal Surfaces, (IJMER), **Vol. 7**, January 2017.

12-A. Picard and H. Fang. Methods to determine water vapour sorption on mass standards, Metrologia, 41 (2004) 333–339.

13- H. Fujiwara, Spectroscopic Ellipsometry: Principles and Applications , John Wiley & Sons,2007.

14-D.H.Goldstein.Polarized light, third edition, CRCPress, Taylor&Francis Grroup (2011).

15- International Organization of Legal Metrology OIML R111-1, Ed. (2004).

16-*R. Schwartz*, Precision Determination of Adsorption Layers on Stainless Steel Mass Standards by Mass Comparison and Ellipsometry: Part I: Adsorption Isotherms in Air, Metrologia, **31** (1994) 117-128.

17- R Schwartz and M Glaser, Procedures for Cleaning Stainless Steel Weights, Investigated by Mass Comparison and Ellipsometry, Meas. Sci, Technol. **5** (1994) 1429-1435.